

Data Analysis:

Figure 1 shows the atmospheric CO₂ concentration measured weekly at the Mauna Loa Observatory (see Ref.1) for the period 29 March 1958 to 08 August 2020. The Observatory is at Latitude 19.54° North, Longitude 155.57° West, Elevation 3397 metres. It is on the northern slope of Mauna Loa, an active volcano on the island of Hawai'i in the mid-North Pacific Ocean.

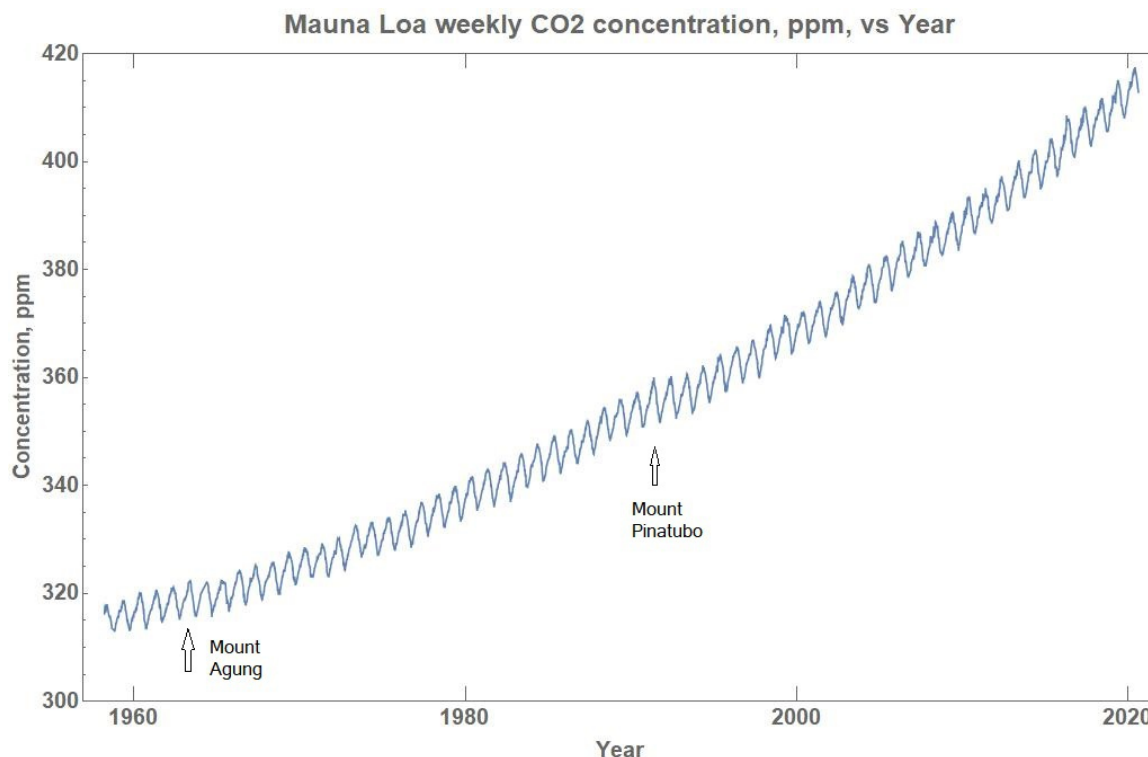


Figure 1. Mauna Loa weekly CO₂ concentration

As there were missing values in the time sequence, interpolation was applied using a third order polynomial fit to adjoining data strings and a 'weekly' time interval of 7.02416 days, that is, one fifty second part of a year, for the following analysis of the CO₂ concentration time series. The original time series consisted of 3183 values while the interpolated time series consisted of 3243 values at a uniform 'weekly' interval.

The series shows a regular seasonal variation superimposed on an upward trend. The linear trend for the whole period of 62 years was 1.58 ppm per annum. For the 3 year period 29 March, 1958 to 1961, the rate was 0.55 ppm pa. For the 3 year period June 2017 to 2020, the rate had steadily increased to 3.08 ppm pa. For the 3 year period July 2017 to 2020, the rate was 3.31 ppm pa and for the 3 year period August 2017 to 2020, the rate was 3.34 ppm pa, more than six times greater than 60 years earlier. The acceleration in the rate of generation of CO₂ over the time of the measurements is attributed to an increase in biogenic CO₂ in response to the gradual increase in temperature since the end of the Little Ice Age. Justification for this claim can be seen in a comparison between the dearth of life at the cold Poles and the profusion of life, in a myriad of forms, in the warm Equatorial zone. Life forms flourish with greater temperature.

There are two inflections in the graph corresponding to the time of the volcanic eruptions at Mount Agung, Bali, Indonesia, 17 March and 16 May, 1963, and Mount Pinatubo, Philippines, 12 June 1991. The increase in the CO₂ concentration appears to have ceased, presumably due to the ash cloud diminishing the Sun's radiation and the consequent photosynthesis and temperature at the Earth's surface. The Mauna Loa Observatory is 9598 km on a bearing of 71° East from

Mount Agung and 8859 km on a bearing of 72° East from Mount Pinatubo. These events contrast with the lack of any change in the accelerating rate of increase of CO_2 during the reduction of economic activity from the 2020 pandemic bringing into question the claim that CO_2 has been increasing due to the activities of mankind.

The amplitude of the seasonal variation ranged from 5.9 ppm early in the series to 9.3 ppm in the later part of the series, changing from year to year in an irregular fashion but clearly increasing in amplitude over time. The maximum in the seasonal variation occurred on average in mid-May at the start of Summer while the minimum occurred at the end of September, just prior to Winter. This is attributed to the Summer sunshine causing an increase in photosynthesis which absorbs CO_2 resulting in the fall in CO_2 concentration. The decay of vegetation in the cold of Winter releases CO_2 resulting in a rise in the CO_2 concentration. That is, the concentration is decreasing during the heat of Summer and increasing during the cool of Winter putting it at odds with the UN IPCC claim that an increase in CO_2 concentration causes a temperature increase.

The annual rate of change of the CO_2 concentration was determined from the interpolated 'weekly' time series by taking the difference between values 52 weeks apart and is shown in Figure 2. It displays the estimated annual rate of change of the CO_2 concentration with high frequency noise superimposed on a cyclic pattern with a linear trend of 0.0286 ppm pa per annum. The sequence of maxima and minima match that for the Oceanic Niño 3.4 Index (Ref.2).

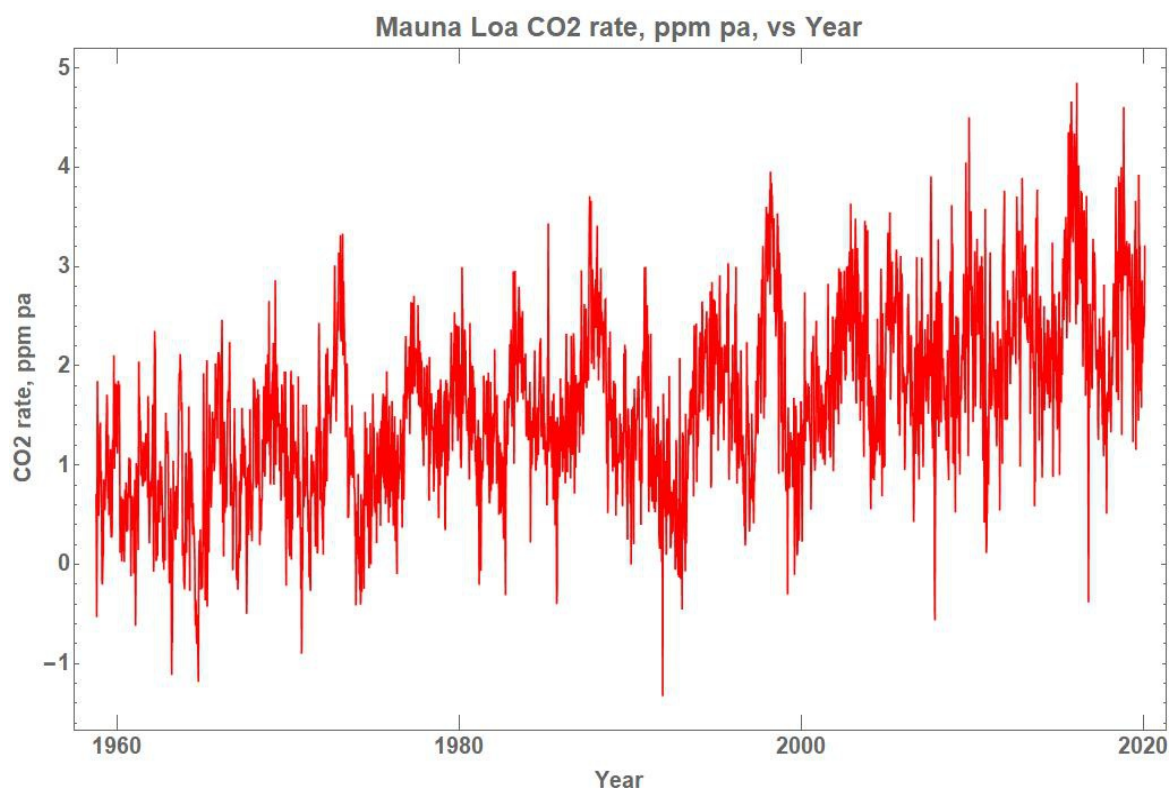


Figure 2. Mauna Loa annual rate of change of CO_2 concentration.

In order to illustrate the correlation between the two series, Figure 3 shows the detrended Mauna Loa annual rate of change of CO_2 concentration, after smoothing with a low pass filter, overlain on the Oceanic Niño 3.4 Index, both covering the same 61 year period. In considering the relationship between the two series it is necessary to be aware that the Mauna Loa rate of change was derived from a weekly series of measurements taken at a single point on the globe. The Oceanic Niño 3.4 Index is the anomaly in the sea surface temperature relative to a 30 year average over the Equatorial zone between latitudes 5° South to 5° North and longitudes 120° West to 170°

West, an area of the central Pacific Ocean of 6,568,670 square kilometres. The Mauna Loa Observatory is 2,450 km from the centre of the Niño 3.4 area, on a bearing of 27.5° East of North.

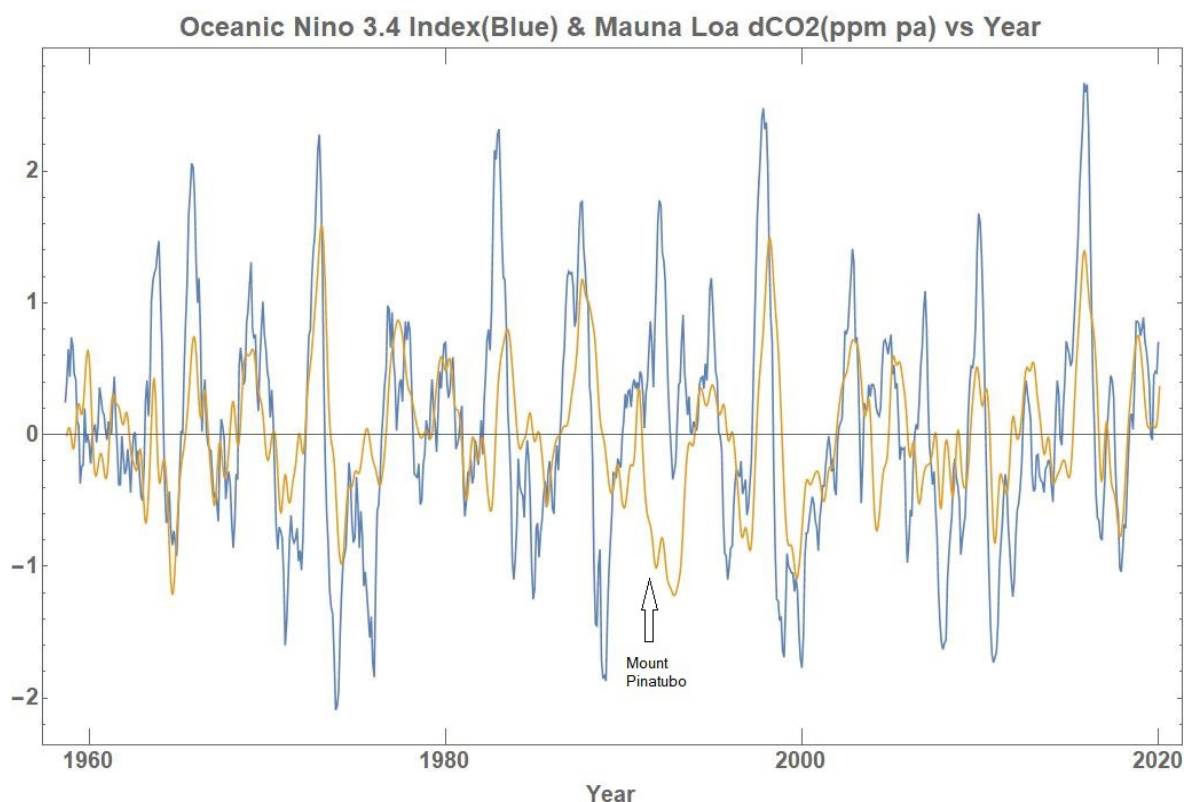


Figure 3. Overlay of the Oceanic Niño 3.4 Index and the Mauna Loa smoothed, detrended CO₂ annual rate of change.

As has been demonstrated in earlier studies of CO₂ data on the accompanying web pages, their seasonal variation has been attributed to biological sources in response to the associated temperature change. Likewise the close correlation between the Mauna Loa CO₂ rate of change and the Oceanic Niño 3.4 Index, as shown by the coincidence of the major maxima in Figure 3, is attributed to a biological response to the major, world-wide climate event depicted by the Niño 3.4 Index.

There is a marked negative correlation in the centre of the graph annotated by ‘↑’ corresponding to the major volcanic eruption of Mount Pinatubo in the Philippines on 12 June 1991 which significantly altered the relationship between the rate of change of CO₂ and the Oceanic Niño 3.4 Index. The eruption caused the rate of change of CO₂ to drop to a minimum as the sea surface temperatures reached a local maximum. The eruption may not have been reflected in the ONI 3.4 sea surface temperatures as Mount Pinatubo is 1675 km North of the Equator.

Autocorrelation Function:

More detail of the source of variation in the CO₂ annual rate of change is shown by its autocorrelation function illustrated in Figure 5. It reveals a clear cyclic pattern based on the El Niño event as shown in the accompanying table listing the correlation maxima, Table 1.

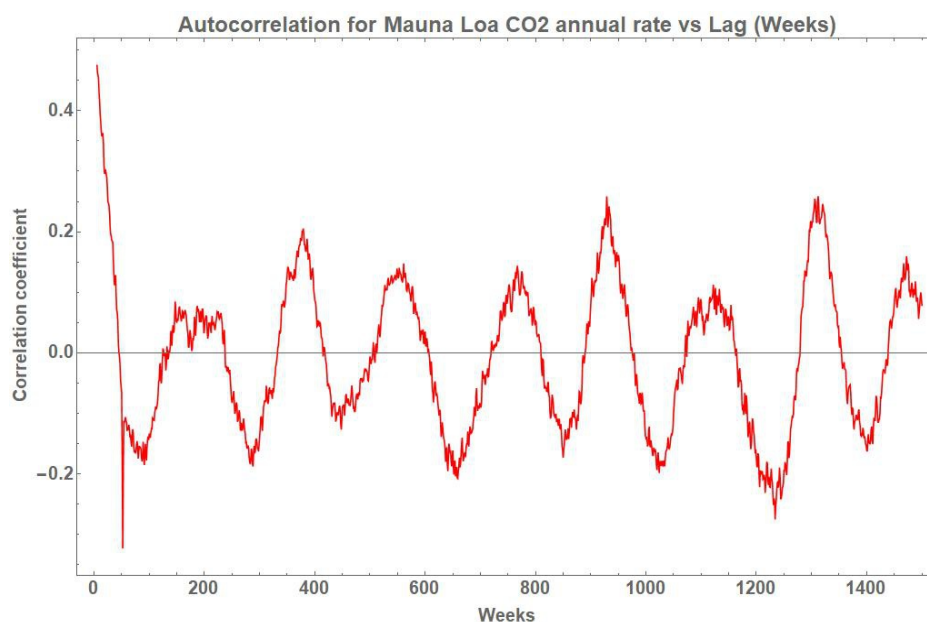


Figure 4. Autocorrelation for CO₂ annual rate of change.

Table 1. Autocorrelation maxima

Amplitude	Years	Weeks	Days	Source
0.076	2.98	155.5	1089	pre-El Niño
0.078	3.60	187.6	1314	El Niño
0.069	4.33	225.8	1580	post-El Niño
0.205	7.29	380.3	2662	2 x El Niño
0.141	10.63	554.9	3884	3 x El Niño
0.144	14.75	769.6	5388	4 x El Niño
0.258	17.87	932.2	6525	5 x El Niño
0.113	21.58	1125.9	7881	6 x El Niño
0.254	25.12	1310.5	9174	7 x El Niño
0.160	28.31	1477.1	10340	8 x El Niño

The average from Table 1, column 4, adjusted for the multiple expressions of the El Niño event was 1313 days. The event clearly dominates the CO₂ annual rate of change indicating that this major climate event together with the seasonal weather pattern determines the rate of generation of CO₂ in the Equatorial region. This confirms the earlier proposition that the temperature level determines the rate of change of CO₂ concentration seen in the monthly data for Cape Grim and Macquarie Island stations and Mt Waliguan Observatory described in the analysis of data from each site as reported in the pages of: <https://www.climateauditor.com>.

Discrete Fourier Transform:

Figure 6 shows the amplitude spectrum from the Discrete Fourier Transform of the interpolated time series for the annual rate of change of the CO₂ concentration padded with zeros at each end to give of length of 4096 values. The amplitude scale was clipped to better display the higher frequency, shorter wavelength events so it excludes the maximum of 9.4 at x-coordinate 22, equivalent to a period of 1308 days, which dominated the autocorrelation function. That is the maximum predicted to represent the response to the El Niño event already seen in the autocorrelation function.

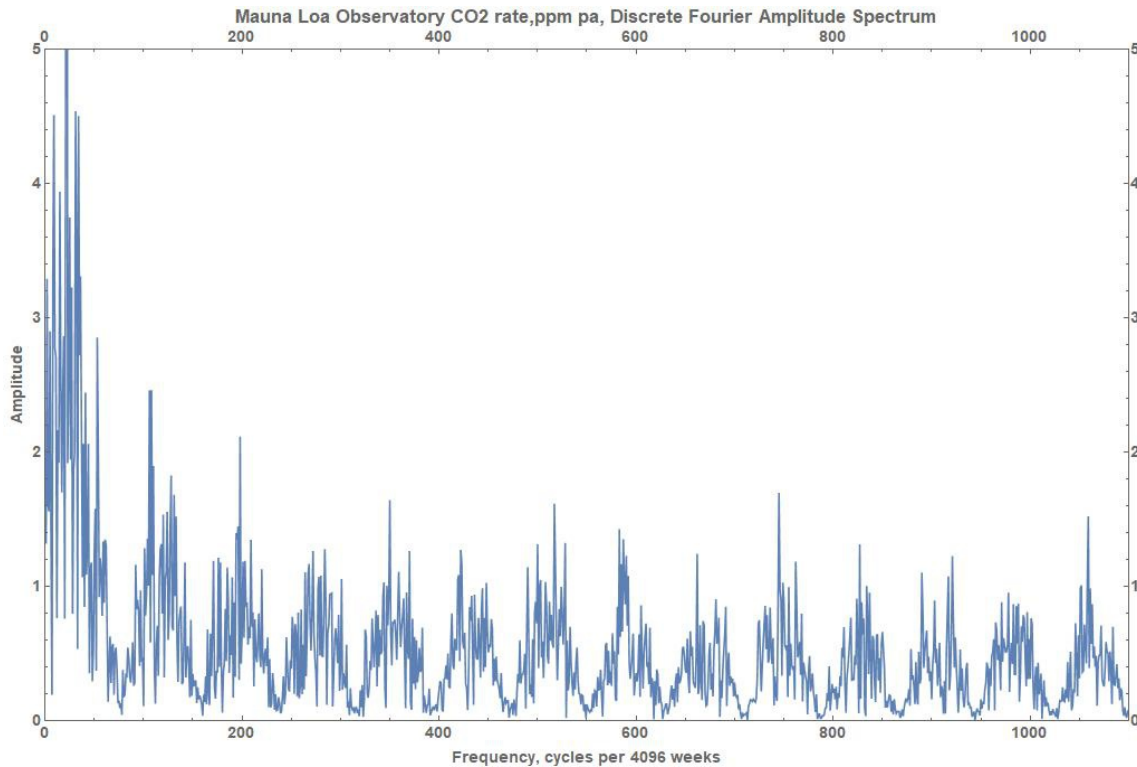


Figure 5. DFT Amplitude spectrum of the annual rate of change of CO₂ concentration.

There is a multitude of local maxima in the Amplitude spectrum some of which have been assigned possible sources from the known synodic periods of the Moon and planets within the Solar System, being the time interval between instances of the Sun, Earth and a planet being in alignment. Average values for these periods have been taken from the publicly available literature but may change with time. The periods drift due to the ever changing configuration of the Solar System and this may contribute to a broadening of the spectral responses. There are other periodic events, such as changes in the ellipticity of the orbits which have not been taken into account in this study.

A list of possible sources is shown in Table 2 for a selection of the peaks in the DFT amplitude spectrum. They are listed by the coordinate on the x axis, in cycles per 4096 weeks, and the amplitude of response with period in years and days for ease of reference to orbital periods of the Moon and planets, e.g. x-coord 2 is 2 cycles in 4096 weeks which is one cycle in 2048 weeks which is a period of 39.38 years or 14,385 days.

Table 2

x-coord	Amplitude	Years	Days	Possible source
2	3.27	39.38	14385	36 x Jupiter synodic, 38 x Saturn synodic
9	4.51	8.75	3197	4 x Mars synodic, 8 x Jupiter synodic
15	3.92	5.25	1918	65 x Moon synodic, 5 x Saturn synodic
22	9.39	3.58	1308	El Niño, 48 x Moon draconic
31	4.56	2.54	928.1	8 x Mercury synodic
34	4.51	2.32	846.2	Mars synodic
53	2.87	1.49	542.8	20 x Moon draconic, Venus synodic
92	1.14	0.86	312.7	
106	2.47	0.74	271.4	10 x Moon draconic
108	2.44	0.73	266.4	9 x Moon synodic
128	1.83	0.62	224.8	8.5 x Moon draconic, 2 x Mercury synodic
176	1.21	0.45	163.47	6 x Moon draconic
196	1.45	0.40	146.79	5 x Moon synodic
209	1.34	0.38	137.66	5 x Moon draconic
220	1.11	0.36	130.78	

268	1.19	0.29	107.35	4 x Moon draconic
284	1.26	0.28	101.31	
350	1.64	0.23	82.20	3 x Moon draconic
370	1.27	0.21	77.76	
422	1.28	0.19	68.18	2.5 x Moon draconic
448	1.01	0.18	64.22	
490	1.16	0.16	58.72	2 x Moon synodic
517	1.63	0.15	55.65	
524	1.00	0.15	54.91	2 x Moon draconic
587	1.36	0.13	49.01	
691	0.84	0.11	41.64	1.5 x Moon draconic
745	1.70	0.11	38.62	
978	0.95	0.08	29.42	Moon synodic
1059	1.51	0.07	27.17	Moon draconic

Some of these may also relate to the periodicities resulting from the Short-term orbital forcing described in Cionco, R. G., and Soon, W. W.-H. [Ref. 3].

Conclusion:

The major influence on the rate of generation of atmospheric CO₂ in the Equatorial zone has been the El Niño event, that is, climate change causing a change in the rate of generation of CO₂, the complete opposite to the UN IPCC claim that CO₂ causes climate change. As far as is known, no physical process has been proposed whereby the CO₂ change could cause an El Niño event.

Furthermore it is notable that both the synodic and draconic periods of the Moon are apparent throughout the 62 year weekly series. An explanation for the synodic period is that each New Moon reduces the incoming Sun's radiation to the Earth and its atmosphere as it passes between the Sun and the Earth. Similar temperature minima must occur when Mercury and/or Venus pass between the Sun and the Earth.

The draconic period is due to the Moon's elliptical plane being at an angle of 5.14° to the Earth's elliptic relative to the Sun. As a result, when the Moon passes through one of the two nodal points, where the Moon's ellipse intersects the Earth's elliptic, it has the greatest influence in diminishing the irradiation of the Earth which, in turn, reduces the Earth's surface temperature thereby causing a response in the rate of generation of CO₂.

Except during a Solar eclipse when the drop in temperature is marked, the passing of the Moon through its nodal points may only causes a minor drop in temperature. In spite of this, there is a measurable effect on the rate of change of CO₂ concentration apparent in the amplitude spectrum implying a significant sensitivity between temperature and CO₂ rate of change. This action appears to have been completely overlooked by the UN IPCC in their assessment of the forces generating the Earth's climate.

As a number of the spectral maxima approximately correspond with the synodic periods of the Moon and the planets, the results are interpreted as showing that the Sun's irradiance of the Earth is modulated by the movement of the Moon and planets. This must cause corresponding changes in the Earth's atmospheric temperature which, in turn, has caused changes in the CO₂ concentration. This is contrary to the never-proven claim by the UN IPCC that increased CO₂ concentration causes an increase in the Earth's atmospheric temperature.

The IPCC First Assessment Report, 1990, consists of this IPCC Overview, quote:

This Overview reflects the conclusions of the reports of (i) the three IPCC Working Groups on science, impacts, and response strategies, and (ii) the Policymaker Summaries of the IPCC Working Groups and the IPCC Special Committee on the Participation of Developing Countries.

1. Science

This section is structured similarly to the Policymaker Summary of Working Group I.

1.0.1 We are certain of the following:

- There is a natural greenhouse effect which already keeps the Earth warmer than it would otherwise be.

- Emissions resulting from human activities are substantially increasing the atmospheric concentrations of the greenhouse gases: carbon dioxide, methane, chloro-fluorocarbons (CFCs) and nitrous oxide. These increases will enhance the greenhouse effect, resulting on average in an additional warming of the Earth's surface. The main greenhouse gas, water vapour, will increase in response to global warming and further enhance it.

End quote.

Both of the above claims appear to have no scientific basis. The first claim is shown to be untenable in the opening page of this web site, entitled “Greenhouse Effect”. The second claim is also untenable as no could know, to this day, all of the possible sources and sinks for the Earth’s atmospheric CO₂. To claim that “Emissions resulting from human activities are substantially increasing the atmospheric concentrations ...” is at odds with the most recent measurements from the Mauna Loa Observatory. For the first 12 days of August 2020, the concentration was on average 2.56 ppm greater than for August 2019.

References:

1. https://scrippsco2.ucsd.edu/data/atmospheric_co2/mlo.html
File: weekly_in_situ_co2_mlo.csv for the period 29 March 1958 to 30 May 2020 plus weekly averages of daily data from Twitter at <https://scripps.ucsd.edu/programs/keelingcurve/> for June, July, August 2020.
2. Oceanic Nino Index, National Oceanic and Atmospheric Administration.
https://www.cpc.ncep.noaa.gov/products/analysis_monitoring/ensostuff/detrend.nino34.ascii.txt
3. Cionco and Soon, Short-term orbital forcing: A quasi-review and a reappraisal of realistic boundary conditions for climate modeling, Earth-Science Reviews 166 (2017) 206-222, Elsevier B.V.